Theoretical Analyses of the Morphological Development of the Hydrogen Bond Network in Protonated Methanol Clusters†

Jer-Lai Kuo,*,‡ Asuka Fujii,*,§ and Naohiko Mikami§

School of Physical and Mathematical Sciences, Nanyang Technological University, 1 Nanyang Walk, Block 5, Level 3, Singapore 637616, Singapore, and Department of Chemistry, Graduate School of Science, Tohoku University, Sendai 980-8578, Japan

Received: June 16, 2007

Extensive density functional theory (DFT) calculations are carried out on various structural isomers of protonated methanol clusters, $H^+(MeOH)_n$ ($n = 2-9$), to analyze the morphological development of the hydrogen bond network in the clusters with an increase of the cluster size. Coexistence of multiple structural isomers is demonstrated by the nearly degenerated energies. Moreover, significant temperature dependence of the preferential isomer structure is shown by the calculated Gibbs free energies. The previously reported infrared spectra of $H^+(MeOH)_n$ (*J. Phys. Chem. A* **2005**, *109*, 138) are revisited on the basis of the spectral simulations of the isomers by DFT calculations.

Introduction

Size-dependent morphological development of hydrogen bond networks in molecular clusters has attracted much interest in the last two decades.[1−6] The collaboration of infrared (IR) spectroscopy and quantum chemical calculations is an especially powerful approach to this issue, and it enables us to directly probe detailed geometric structures of microscopic hydrogen bond networks. Protonated water clusters, $H^+(H_2O)_n$, are the most extensively studied systems because of their fundamental importance as a model of the proton solvation.[5−15] Their morphological development process from the simple chain type structures at the small sizes to the characteristic polyhedral cage formation in the large size has been elucidated. Identification of the protonated core structure, the Eigen (H_3O^+) or Zundel ($H_5O_2^+$) type, has also been recently carried out by the direct observation of the ion core vibrations.[16]

Methanol (MeOH) is one of the most important protic solvents, and its hydrogen bond network structure can be a prototype to understand those of alcohols.[17−19] Moreover, proton solvation structures and identification of the protonated core type (analogue to the Eigen type, $CH_3OH_2^+$, or that of the Zundel type, $CH_3OH-H^+-HOCH_3$) in protonated methanol are important alternatives to those of water to establish a microscopic picture of the proton solvation. However, structural studies on protonated methanol clusters, $H^+(MeOH)_n$, have been much scarce in comparison with the recent extensive studies on protonated water clusters.[20−23] Because the maximum coordination number of methanol is three, much simpler network structures than those of water are expected. Therefore, protonated methanol clusters would be able to provide us a more unequivocal example for understanding of morphological development in a hydrogen-bonded molecular system.

Mass spectrometry of $H^+(MeOH)_n$ was carried out by Zhang et al. up to the size of $n = 24$.[20] In contrast with the case of $H^+(H_2O)_n$,[24,25] no magic number was found for $H^+(MeOH)_n$, suggesting morphological development without a specific "closed shell" structure. IR spectroscopy was first applied by Chang et al. to $n = 4$ and 5.[21,22] While the linear chain structure was determined for $n = 4$, coexistence of the linear chain and cyclic structural isomers was demonstrated for $n = 5$ on the basis of the temperature dependence of the IR spectra and the density functional theory (DFT) calculations. They proposed a specific proton-transfer mechanism in $H^+(MeOH)_n$ by the transformation between the linear chain and cyclic structures. Then, IR spectroscopy of the larger-sized clusters was reported by Fujii et al. up to $n = 15$.[23] Morphological development of the hydrogen bond network structure was examined when considering the topological nature of the hydrogen bond coordination in methanol, and the termination of the morphological development with the formation of "bicyclic" structures at $n = 7$ was concluded. Though this conclusion was qualitatively supported with the dangling (free) OH stretch band behavior in the observed IR spectra, no extensive theoretical calculations have been carried out to quantitatively test this conclusion.

In this paper, we report extensive DFT calculations of $H^+(MeOH)_n$ to examine its morphological development process. We calculate the energy-optimized structures, relative potential energies including the zero-point energy (ZPE) corrections and Gibbs free energies for more than 100 isomers of $H^+(MeOH)_n$ ($n = 2-9$). It is shown that the ZPE correction is important for precise evaluation of the relative energies of structural isomers. Moreover, significant temperature dependence of the relative free energy is found, and coexistence of multiple structural isomers is expected at the experimental temperature. We revisit the previously observed IR spectra of $H^+(MeOH)_n$[23] with the spectral simulations on the basis of the energy-optimized isomer structures and examine the morphological development of the hydrogen bond network structure with the cluster size.

Computations

Geometries of $H^+(MeOH)_n$ ($n = 2-9$) are fully optimized at the B3LYP/6-31+G* level using the Gaussian 03 program

† Part of the "Sheng Hsien Lin Festschrift".

* Corresponding authors. E-mail: (J.-L.K) JLKuo@ntu.edu.sg; (A.F.) asukafujii@mail.tains.tohoku.ac.jp.

‡ Nanyang Technological University.

§ Tohoku University.

10.1021/jp074676t CCC: $37.00
Published on Web 08/08/2007

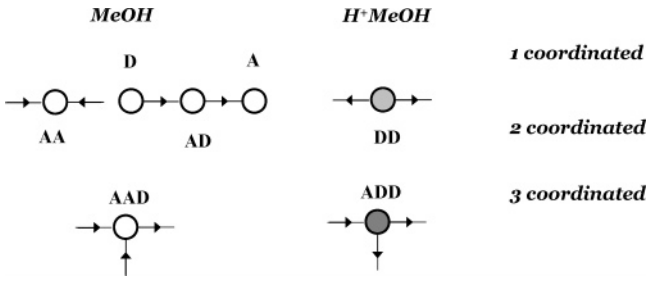

Figure 1. Symbolic representations of the possible coordination types of the MeOH and H^+MeOH sites (ref 23). All the methyl groups and hydrogen atoms are omitted in this representation. The oxygen atom on MeOH is represented by an open circle and the oxygen atom on H^+MeOH is shown as a gray circle. An arrow indicates a hydrogen bond that binds two oxygen atoms. The direction of the arrow shows the donor−acceptor relation in the hydrogen bond.

package.[26] ZPE is also calculated under the harmonic approximation at the same level. Regarding the use of the B3LYP/6-31+G* level of calculations, this level has been extensively employed in the studies on protonated hydrogen-bonded clusters by Chang and co-workers, and it has successfully reproduced experimental observations.[27−30] To access the thermal effects, we also calculate the Gibbs free energy at 190 K, which is in the middle of the estimated experimental temperature of the previously reported IR spectra.[8,10,23]

Coordination Types of MeOH and H^+MeOH Sites

Prior to detailed descriptions on the energy-optimized isomer structures of $H^+(MeOH)_n$, we shall briefly summarize the possible coordination types of MeOH and H^+MeOH sites and morphology types of $H^+(MeOH)_n$. These are very useful to understand the morphological feature in the hydrogen bond network of $H^+(MeOH)_n$, and have been first introduced in our previous paper to qualitatively interpret the observed IR spectra of $H^+(MeOH)_n$.[23]

Figure 1 shows the symbolic representations of the possible coordination types for the MeOH and H^+MeOH sites according to their coordination numbers. On one-coordinated sites, a MeOH can either be an A (proton acceptor) or a D (proton donor) site. On two-coordinated sites, a MeOH can take the form of an AA (double acceptor) or an AD (single acceptor single donor). A three-coordinated site of a MeOH is uniquely an AAD (double acceptor single donor). Different from the case of water, an ADD (single acceptor double donor) site is prohibited for a MeOH because of the lack of the second proton to donate.

On first sight, the coordination type for a H^+MeOH seems to be more complicated than (or at least comparable to) that of a MeOH molecule, but it is not true. Though it is geometrically acceptable for a H^+MeOH to be a one-coordinated A or D site and a two-coordinated AD or AA site, it is easy to understand such coordination types are energetically not favorable (except for very small cluster sizes) as the hydrogen bonds between the ion-core and neighboring MeOH molecules are stronger than the hydrogen bonds between two neutral MeOH molecules (as a result, the ion-core would like to donate both of its protons). This tendency has been verified earlier by Chang and co-workers.[21,22] Following this empirical rule, we conclude that the coordination type of a H^+MeOH should be either a two-coordinated DD (double donor) site or a three-coordinated ADD (single acceptor double donor) site. However, in the extensive calculations of energy-optimized structures of various protonated clusters, we found that the latter form is not stable: even in the large $H^+(H_2O)_m(MeOH)_1$ clusters (up to $m = 20$) of the cage morphology (where almost all the molecules are three-coordinated), no stable ADD site of H^+MeOH was found.[30] In the present study, we have also attempted to construct many $H^+(MeOH)_n$ isomers that initially contain the ADD site of H^+-MeOH, but none of these structures remains as a stable local minimum upon the geometry optimization.

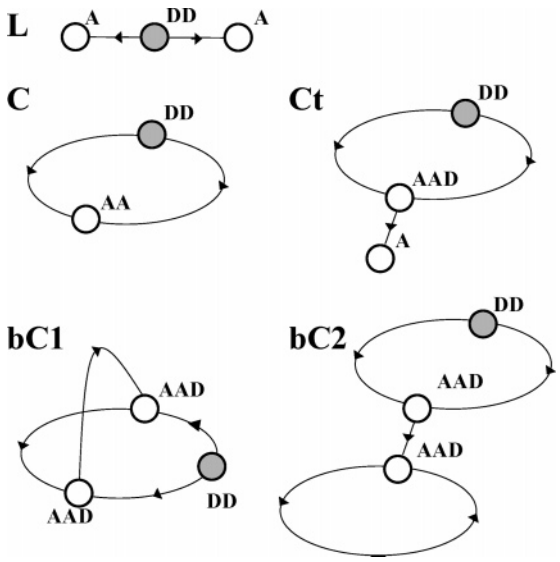

Figure 2. Schematic representations of the five basic morphologies of $H^+(MeOH)_n$. The same conventions for simplification as those used in Figure 1 are adapted here. In addition, all the AD molecules are neglected in the representations for simplicity.

Morphological Development of $H^+(MeOH)_n$

With the coordination types discussed above, one can construct only five basic types (L, linear, C, cyclic, Ct, cyclic with a tail, bC1, first type of bicyclic, and bC2, second type of bicyclic) of morphologies for $H^+(MeOH)_n$,[23] and they are schematically shown in Figure 2. It should be noted that for simplicity, all the AD molecules are neglected in the schematic representations of Figure 2. Any of the lines in the representations can be extended by adding more AD molecules. Other than that, the only possible extension is to add linear side chains from the AD sites. Such a side chain is, however, terminated by a D site, and the terminal D site cannot be bound to any site to form further ring structures.

L. Linear (L) structures are the most basic form of $H^+(MeOH)_n$, and they exist for $n \geq 2$. Among the many possible positions for the excess proton to reside, we found that the excess proton prefers to stay at the center of the hydrogen bond network. As a result, there is an interesting alternation of the ion-core form between the Zundel type (n = even) and the Eigen type (n = odd). Similar alternation has been confirmed for protonated ethanol clusters.[31] The most stable L structures of $H^+(MeOH)_n$ are shown in Figure 3 as Ln.

C and Ct. When a terminal molecule (A site) of a linear structure is bound to any site in the hydrogen-bonded line, a cyclic structure is formed. Such a simple cyclic structure can be divided into two categories. In the first kind, two terminal molecules are bound to each other. The binding site becomes an AA site. In the second categories, the hydrogen bond network in the ring is further extended by branching out a "tail" from the AA site. Then, the branching site becomes an AAD site, and the tail is terminated by an A site. In the following, we will refer the first kind as C and the second kind is called Ct. While it is straightforward to build the structures of these cyclic isomers, there are also many variations of the relative positions

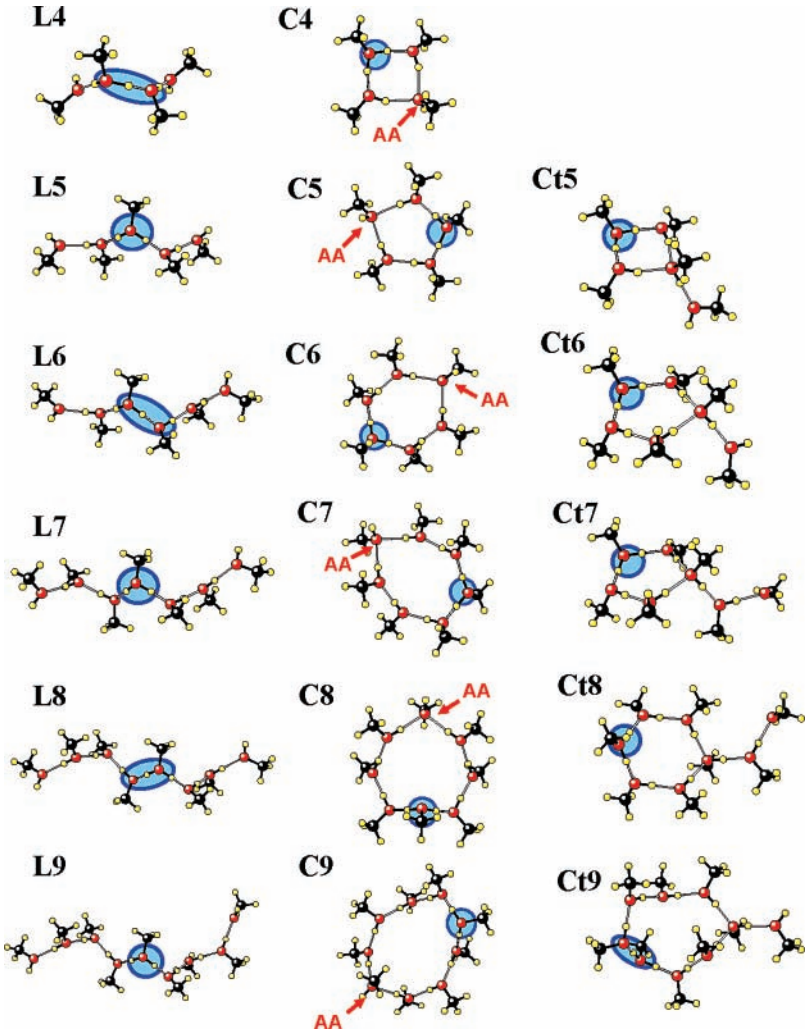

Figure 3. The most stable structures of the L*n*, C*n*, and Ct*n* up to $n = 9$. The positions of the ion-core (either H^+MeOH or $H^+(MeOH)_2$) are highlighted with the blue circles.

of the DD and AA (in C) or AAD (in Ct) sites. We investigated all the possible configurations and found that DD and AA in C prefer to be separated as far as they could. The most stable structures of C and Ct are also shown in Figure 3. The C and Ct morphologies are found to be stable only in $n \geq 4$ and $n \geq 5$, respectively. This is consistent with the previous report by Chang et al. on the small-sized C clusters.[21,22]

These basic forms can be further extended by adding side chains, which are necessarily terminated by a D site. We also attempted to add side chain(s) to all these three basic morphologies. The smallest sizes of L*ns* [L with D-terminated side chain(s)], C*ns* [C with D-terminated side chain(s)], and Ct*ns* [Ct with D-terminated side chain(s)] are found at $n = 6$. As we described in the previous subsection, the side chain(s) cannot be added on the ion-core and its immediate neighbors. But up to $n = 9$, we have found that these structures with D-terminated side chain(s) are energetically unfavorable comparing to their generic forms.

A common feature to these three basic morphologies described above is that the hydrogen bond networks are terminated by a MeOH with a dangling (free) OH group (A or AA). When all the dangling OH groups are hydrogen-bonded, the morphology develops into another group, bC1 and bC2, of compact structures. They correspond to the bicyclic structures in the nomenclature in our previous paper on $H^+(MeOH)_n$.[23] From a structural (not topological) point of view, we can further divide bC1 into two groups. In bC1a, the shortest hydrogen bond network directly connects the two three-coordinated (AAD) molecules without any AD molecules in between them. In bC1b, all three hydrogen bond lines have at least one AD molecules. The most stable forms in each category is compiled and shown in Figure 4.

bC1a and bC1b. These are the most compact structure with the largest number of hydrogen bonds among the morphologies of the clusters of the same size. No more complicated structures can be formed, and in this meaning this morphology is the terminal of the morphological development in $H^+(MeOH)_n$. In the previous experimental report,[23] bC1 structures have been expected to be formed in $n \geq 7$ on the basis of the qualitative discussion on the morphological development of $H^+(MeOH)_n$. The minimum sizes for the stable bC1a and bC1b structures, however, are found to be $n = 6$ and $n = 5$, respectively, in the present DFT calculations. This is because the three- and four-member rings, which have not yet been experimentally confirmed for $H^+(MeOH)_n$,[21−23] were ignored in our previous qualitative discussion. As the size of the cluster grows, there are more structural isomers of the bC1 type. For example, in bC1a8 in addition to the most stable (six-member ring + four-member ring) isomer, one can easily think of another isomer containing two five-member rings. We examined many different conformations in each cluster size and found the clear preference for the ion-core to reside on the larger size ring. This is because the larger ring can release the greater strain than the smaller ring, and it is more effective to stabilize the energy for the strong

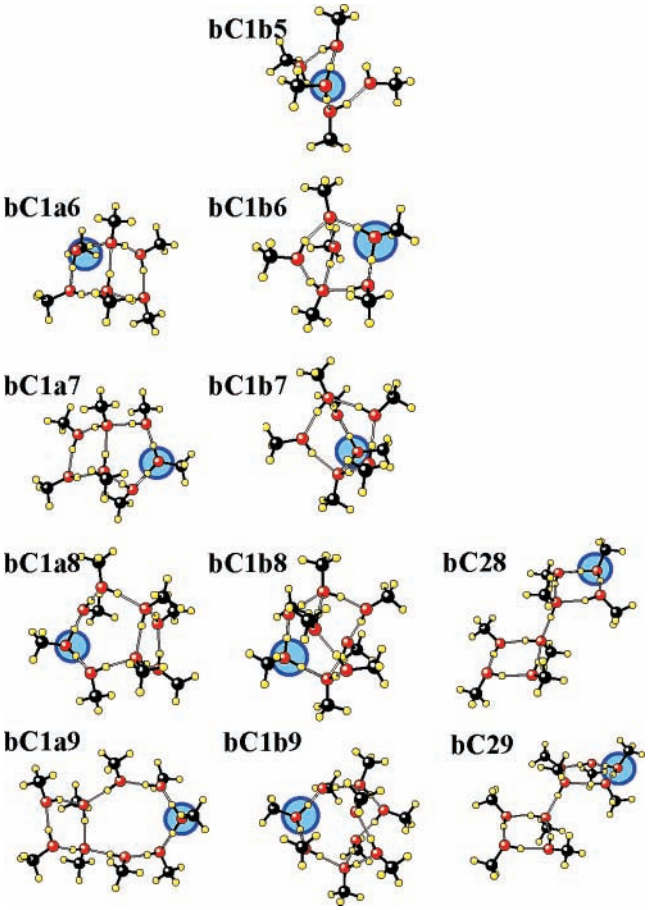

Figure 4. The most stable structures of the bC1a*n*, bC1b*n* and bC2*n* up to $n = 9$. The positions of the ion-core are highlighted with the blue circles.

hydrogen bonds around the ion core. The same preference for the ion-core to reside on the largest sized ring is evident also for the bC1b type structures, as seen in Figure 4.

bC2. Various stable forms of bC2*n* were found and the smallest one is bC28. A bC27 structure, which consists of a four-member ring with the ion-core and a three-member ring, cannot be a local minimum upon the geometry optimization. For bC29, there are at least two possible positions for the ion-core, and it turns out that ion-core prefers to stay on the larger ring. This is the same tendency as that seen in the bC1 structures.

Relative Stability

We performed geometry optimization on all the structures of $H^+(MeOH)_m$ shown in Figures 3 and 4 at the B3LYP/6-31+G* level, and the energy data are tabulated in Table 1. The electronic potential energy (E_o) is evaluated after the geometry optimization converges and ZPE is estimated by the standard harmonic approximation.

For better description on the size evolution on the relative stability of the different morphologies, we depicted the relative energies in Figure 5. The difference in E_o spans a range of ~8 kcal/mol (at $n = 9$). As the cluster size increases, the tendency for more "compact" structures (bC2, bC1a, and bC1b) to gain greater binding energy is clear. This trend is in line with the fact that there are more hydrogen bonds in the compact structures in comparison with the "open" structures (L, C, and Ct). The difference in ZPE is ~3 kcal/mol (fairly consistent across all the sizes), and the trend in ΔZPE (favoring the open structures because of the lower vibrational frequencies due to the flexible structures) is just the opposite to the trend in the ΔE_o. The relative stability at 0 K is determined by the competition between ΔE_o and ΔZPE. It is seen in Figure 4c that the compact structures become comparable with the open structures at $n = 7$ or 8.

TABLE 1: B3LYP/6-31+G* Calculated Energies: E_o and ZPE Correction are Given in Hartree[a]

name	E_o	ΔE_o	ZPE	ΔZPE	$\Delta (E_o + \text{ZPE})$	ΔG
L4	−463.31087	**1.04**	0.22163	**0.00**	**−1.61**	**−3.65**
L5	−579.05848	**1.81**	0.27664	**−0.17**	**1.64**	**0.49**
L6	−694.80305	**3.59**	0.32970	**−1.20**	**2.39**	**−0.16**
L7	−810.54651	**5.30**	0.38337	**−2.58**	**2.72**	**−1.27**
L8	−926.28859	**6.46**	0.43637	**−2.53**	**3.93**	**−1.24**
L9	−1042.03021	**7.15**	0.49014	**−2.27**	**4.88**	**0.64**
Ct5	−579.06077	**0.37**	0.27905	**1.35**	**1.72**	**1.39**
Ct6	−694.80877	**0.00**	0.33161	**0.00**	**0.00**	**0.00**
Ct7	−810.55286	**1.32**	0.38509	**−1.50**	**−0.19**	**−2.31**
Ct8	−926.29635	**1.59**	0.43871	**−1.06**	**0.53**	**−1.70**
Ct9	−1042.03717	**2.78**	0.49269	**−0.67**	**2.12**	**1.27**
C4	−463.31252	**0.00**	0.22584	**2.64**	**0.00**	**0.00**
C5	−579.06136	**0.00**	0.27691	**0.00**	**0.00**	**0.00**
C6	−694.80690	**1.17**	0.33183	**0.13**	**1.31**	**1.24**
C7	−810.54993	**3.15**	0.38457	**−1.83**	**1.32**	**−0.79**
C8	−926.28840	**6.58**	0.43774	**−1.67**	**4.92**	**1.91**
C9	−1042.03144	**6.38**	0.49067	**−1.93**	**4.45**	**3.03**
bC28	−926.28856	**6.49**	0.44104	**0.40**	**6.88**	**4.43**
bC29	−1042.03604	**3.49**	0.49317	**−0.36**	**3.13**	**2.25**
bC1a6	−694.80567	**1.95**	0.33373	**1.33**	**3.27**	**4.57**
bC1a7	−810.55496	**0.00**	0.38748	**0.00**	**0.00**	**0.00**
bC1a8	−926.29889	**0.00**	0.44040	**0.00**	**0.00**	**0.00**
bC1a9	−1042.04160	**0.00**	0.49375	**0.00**	**0.00**	**0.00**
bC1b5	−579.05512	**3.92**	0.27981	**1.82**	**5.74**	**6.30**
bC1b6	−694.80878	**0.00**	0.33298	**0.86**	**0.85**	**2.46**
bC1b7	−810.55451	**0.28**	0.38743	**−0.04**	**0.25**	**0.51**
bC1b8	−926.29899	**−0.06**	0.44139	**0.62**	**0.56**	**1.88**
bC1b9	−1042.04182	**−0.14**	0.49511	**0.85**	**0.72**	**2.89**

[a] We also calculated Gibbs free energy (G) at 190 K. The relative quantities [ΔE_o, ΔZPE, $\Delta(E_o + \text{ZPE})$ and ΔG] are shown bold in the unit of kcal/mol. The zero of the relative energies scales is set to be the most stable form of each cluster size.

To access the thermal effects on the relative stability, we also calculated the Gibbs free energy at 190 K [G(190 K)]. The temperature of 190 K is in the middle of the estimated temperature range of the previous spectroscopic experiments of the protonated clusters.[8,10,23] The calculated Gibbs free energy also favors the open structures because of the rich low-frequency modes, and we can see in Figure 4d that the L9 (which is 8 kcal/mol higher in E_o) has comparable Gibbs free energy as those of the compact forms. The differences among the Gibbs free energy of these five basic morphologies are about 2 kcal/mol at 190 K.

We should note here that higher temperature will further favor the free energy of the linear form (or the more open forms in general). The comparison between Figure 5, panels c and d, demonstrates the effects of the thermal energy on alerting the relative stability. In light of the excess thermal energy in the experiment observations, we would expect that the coexistence of the multiple isomers is highly plausible also for the larger clusters. Such expectation of the coexistence of the multiple isomers at a finite temperature is consistent with the observation of no clear magic number in the mass spectrometry of $H^+(MeOH)_n$,[20] in spite of the plausible formation the of the "closed shell" structures, bC1a and bC1b, at $n = 5-6$. More evidence will be shown in the analysis of the vibrational spectra of $H^+(MeOH)_n$.

DFT Calculated Vibrational Spectra

Figure 6 shows the simulated IR spectra on the basis of the energy-optimized structures. All the calculated harmonic frequencies are scaled by a factor of 0.975, which is determined

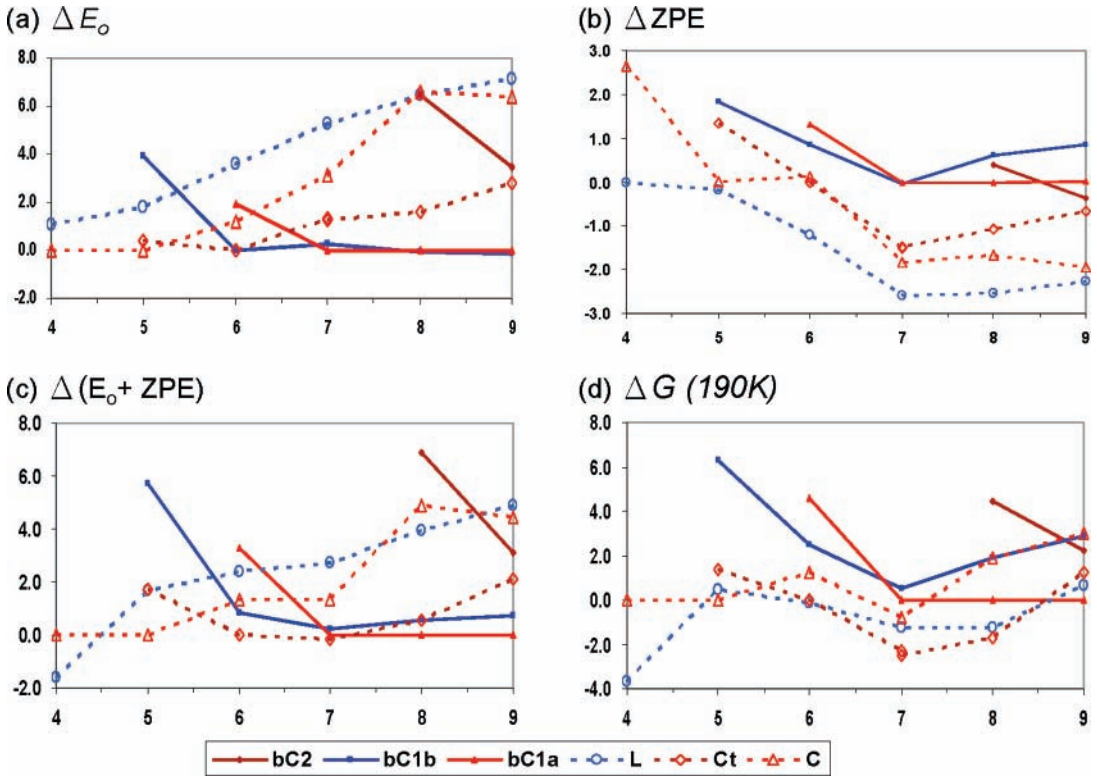

Figure 5. Relative stabilities (in kcal/mol) of the different morphologies of $H^+(MeOH)_n$. The size of the cluster is indicated by the *x*-axis.

to reproduce the free OH-stretch band in pure and protonated water clusters.[7,28] The stick spectrum is converted into the continuous spectrum by the convolution with a Lorentzian function of 10 cm^{-1} full width at half-maximum.

The most distinct feature separating the six types of structures is located slightly below 3700 cm^{-1}, which is assigned to the dangling OH stretching. This vibrational signature is seen only in L, C, and Ct, but is absent for bC2, bC1a, and bC1b.

Another interesting finding in the vibration spectra is that the above-mentioned two groups of morphologies also show rather different trends in the hydrogen-bonded OH stretch bands in the range between 3000 and 3600 cm^{-1}. One can easily find from Figure 6 that the vibrational modes in the first group (L, C, and Ct) show a clear tendency to be blue-shifted as the cluster size increases. The second group (bC2, bC1a, and bC1b) has the opposite trend and their vibrational modes have a tendency to be red-shifted. With an increase of the cluster size, the larger co-operative effects among the hydrogen bonds are ordinarily expected, and it would result in the red shifts of the hydrogen-bonded OH stretch frequencies. The blue shifts in the first group, however, demonstrate the reduction of the hydrogen bond strength, and its origin is attributed to the increase of the average distance from the ion-core. On the other hand, the red-shifts in the second group indicate the enhancement of the hydrogen bond strength. In such a compact structure group, the distortion of the hydrogen bond angle in the ring/cage moieties is reduced with the increase of the size. The similar effect of the size increase has been seen in the IR spectra of neutral $(MeOH)_n$, which have simple cyclic structures.[17]

L. The hydrogen-bonded OH stretching frequencies in the linear clusters show a clear dependency on their distance from the ion-core. The gross band features increase their frequencies from 3050 to 3430 cm^{-1} as the many of hydrogen bonds move away from the ion-core.

C. Two hydrogen bonds adjacent to the AA site also show a slight blue shift tendency when the cluster size increases (as these two hydrogen bonds are further away from the ion core). In $n \geq 6$, an additional group (the second nearest hydrogen bonds to the AA site) also emerges. These two groups stabilize at 3500 and 3350 cm^{-1}, respectively.

Ct. The vibrational signature of Ct is very similar to that of C. For the same reason, the two hydrogen bonds adjacent to the AAD molecule also show a slight blue shift tendency. The difference from the C spectra is the extra feature due to the hydrogen bonds between the AAD and the A molecules. This feature also shows a blue shift tendency.

bC2. One of the two rings consists entirely of neutral MeOH molecules (shown in blue), and their frequency (~3400 cm^{-1}) is fairly close that of neutral $(MeOH)_4$ reported by Buck and Huisken.[17]

bC1a. The vibrational modes in bC1a are delocalized within the whole cluster strucure. This is due to the strong coupling among the local OH oscillators, and the resulting normal modes are not localized on a single hydrogen bond.

bC1b. The vibrational modes show two features. The first group (in blue) comes from the OH stretching of the AD molecules that are not in the vicinity of the ion-core. The second group comes from the ADD molecules. Both groups show red shifts as the size of the hydrogen bond network increases.

Comparison with the Observed Vibrational Spectra

IR spectroscopy of size-selected $H^+(MeOH)_n$ has been pioneered by Chang et al. for $n = 4$ and 5,[21,22] and then we have reported the IR spectra of $n = 4-15$ in the hydrogen-bonded and dangling OH stretch regions.[23] In this subsection, we discuss the band features in the observed IR spectra in comparison with the DFT spectral simulations.

As we discussed in the above sections, the relative population of the structural isomers would strongly depend on the vibrational temperature of the cluster. Because of the large excess energies in the ionization and protonation processes,

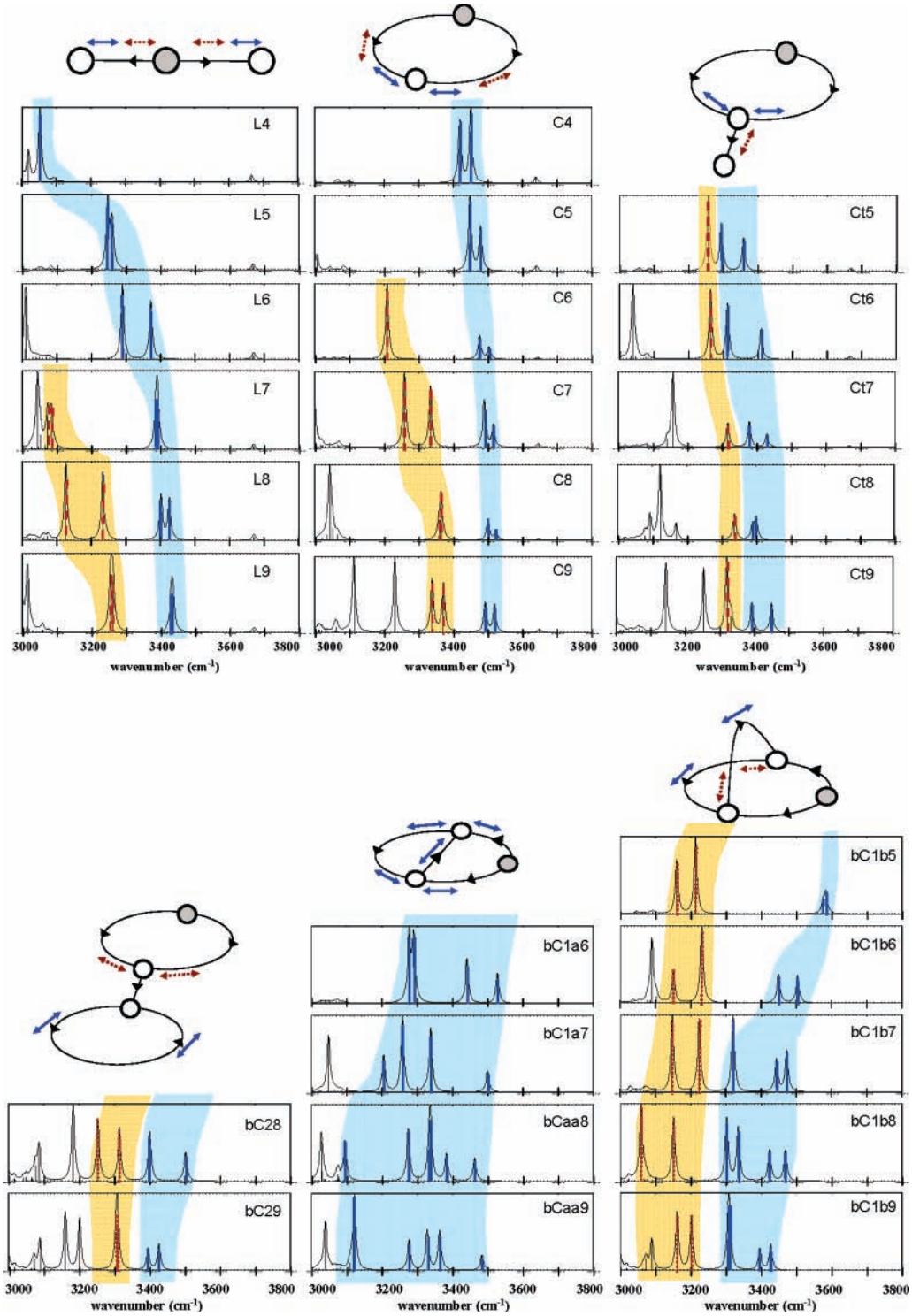

Figure 6. Vibrational spectra of $H^+(MeOH)_n$ calculated by B3LYP/6-31+G* (rescaled by the scaling factor of 0.975). The vibrational modes are color-coded with the vibrational modes shown in the schematic representation of the morphologies, and the stripes are made for eye-guiding purposes.

protonated clusters under the gas-phase spectroscopic observation are more or less thermalized. In our measurement, the $H^+(MeOH)_n$ clusters were prepared by the laser-assisted discharge.[23] Vibrational temperature of $H^+(H_2O)_{21}$ prepared by the same technique is roughly estimated to be 160−200 K by the comparison with the temperature dependence of the dangling OH stretch bands reported by Wu et al.[8,10] Though evaporation cooling efficiency would depend on the cluster size and species, it is reasonable to assume the same vibrational temperature for the observed $H^+(MeOH)_n$ clusters. Then, we employ the free energies of the isomers at 190 K, which are summarized in Table 1 and Figure 5 as a measure of the relative contribution to the observed IR spectra.

The observed IR spectra of $H^+(MeOH)_n$ ($n = 4-12$) in the OH stretch region are shown in Figure 7. These spectra are reproductions of those reported in ref 23. The gap in the spectra at the 3440−3520 cm^{-1} region is due to the absorption of the nonlinear crystal to generate the IR light. Broad features below 3500 cm^{-1} are attributed to hydrogen-bonded OH stretching vibrations, and the relatively sharp band at 3670 cm^{-1} is

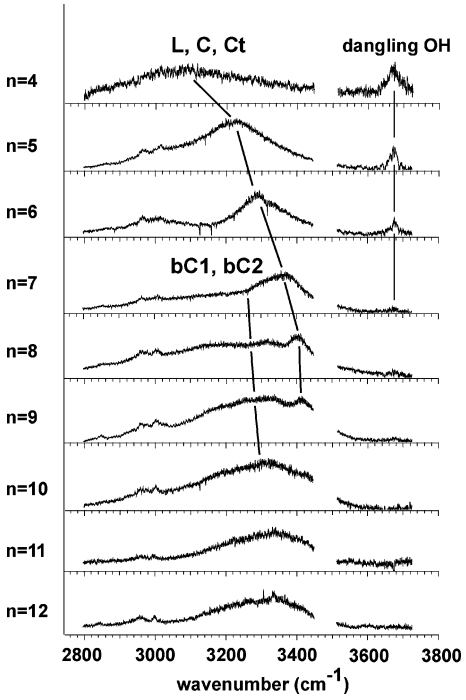

Figure 7. Observed IR spectra of $H^+(MeOH)_n$ ($n = 4-12$). The solid lines indicate the characteristic band features of the isomer structures (see text).

assigned to the dangling OH stretch vibrations. Small shoulders just below 3000 cm^{-1} are due to the CH stretches of the methyl group, and no remarkable size-dependence is found for the CH stretches.

In the observed spectra of $n = 4-8$, the peak position of the broad hydrogen-bonded OH stretch band shows gradual high-frequency shifts with the increase of the clusters size. This blue-shifting feature is seen up to $n = 9$, but its shift almost saturates at $n = 8$. Another broadened feature centered at around 3300 cm^{-1} begins to appear at $n = 7$ as an extremely broadened shoulder of the blue-shifting band. Then, this new band grows with the size, and it becomes the main feature of the spectrum in $n \geq 8$. In $n \geq 10$, all the hydrogen-bonded OH stretch bands finally converge into a single broadened peak centered at 3300 cm^{-1}. On the other hand, the dangling OH stretches form a relatively sharp single peak at 3670 cm^{-1}. Its intensity decreases with the increase of the cluster size, and the dangling OH stretch band almost disappears at $n = 7$.

The blue shift of the hydrogen-bonded OH bands observed in the smaller sizes is the characteristic feature expected for the open structures (L, C, and Ct). The coexistence of L and C isomers in $n = 5$ has been already confirmed by the temperature dependence of the IR spectra by Chang et al.[21,22] The present DFT calculations indicated that in the smallest observed sizes, $n = 4$ and 5, only the open structures are stable or they are much more stable than the compact structures. At $n = 6$, bC1b is the most stable in E_o, but inclusion of the ZPE and Gibbs energy suggests the advantage of the flexible open structure at 190 K. The blue-shifting bands in the hydrogen-bonded OH stretch region well support the dominance of the open structure in the size range of $n = 4-6$. The clear appearance of the dangling OH stretch band is another support for the open structures. At $n = 7$, we observe the disappearance of the dangling OH band and appearance of a new broadened band at around 3300 cm^{-1}. In our previous report of the IR spectra, we discussed the possible isomer structures of $H^+(MeOH)_n$ only with the schematic morphology consideration, and proposed the formation of the bicyclic structures (corresponding to bC1b and bC2 in the present terminology) at $n = 7$, though it was only qualitatively evidenced by the disappearance of the dangling OH stretch band at this size.[23] In accord with the previous qualitative discussion, the present DFT calculations suggest that the contribution of the compact structures, bC1a and bC1b, begins at around this size, when we consider the temperature effect at 190 K. The band position of the new broadened band (at around 3300 cm^{-1}) is also consistent with the DFT predictions, as seen in Figure 6. The remarkable decrease of the dangling OH band intensity is a clear spectral signature for the reduction of the relative population of the open structures. However, the observation of the blue-shifting band at this size demonstrates that the open structures still coexist, as expected by the DFT calculations.

The broadened band due to the compact structures becomes the dominant feature in the larger sizes, and this is an indication of the enhanced relative population of the compact structures. On the other hand, the blue-shifting band also survives at least up to $n = 9$, demonstrating the coexisting the open structures. In $n \geq 7$, the compact structure is much more stable than open structures in E_o, but the remarkable effects of the ZPE and Gibbs free energy make the open structures still competitive with the compact structures at 190 K. The saturation of the magnitude of the blue shift at around $n = 8$ is also consistent with the expectation of the DFT calculations.

All the isomer structures at the large sizes show rich band features in the 3200−3500 cm^{-1} region, and their overlap would wash out the spectral signature of each isomer and result in a single broadened band. No clear size dependence is actually seen in the observed IR spectra of $n \geq 10$, and it supports the coexisting of the multiple isomers at the finite temperature, as was demonstrated in Figure 5.

The qualitative agreement between the observed and simulated spectra is confirmed, demonstrating the reliability of the present DFT calculations. As we described above, however, the entropy effect is very significant in the relative free energy evaluation, and precise evaluation of the vibrational temperature of the cluster is required for more quantitative discussion.

Summary

Extensive DFT calculations at the B3LYP/6-31+G* level were carried out for $H^+(MeOH)_n$ to explore the morphological development of the protonated clusters with the cluster size. The morphological types of $H^+(MeOH)_n$ were categorized and the most stable structure of each category was estimated by the evaluation of the various energy-optimized structures. The DFT calculations showed that the open structures that have dangling OH bonds are most stable in the small sized clusters and the compact structures with the closed hydrogen-bonded rings become most stable in $n \geq 6$. However, the inclusion of the ZPE and Gibbs free energy strongly suggests the coexistence of the multiple isomers of the various morphological types at the finite temperature, demonstrating the significant importance of the temperature effects. The previously reported IR spectra of $H^+(MeOH)_n$ were compared with the spectral simulations on the basis of the DFT calculations. The comparison supported the morphological development and coexistence of the multiple isomers predicted by the DFT calculations.

Acknowledgment. J.L.K. would like to thank Nanyang Technological University for financial support (RG34/05 and RG57/05) and Professor Chien-Cheng Chang for his hospitality during the manuscript preparation at Academia Sinica. This

work was partially supported also by JSPS through the Project No. 19205001 of the Grant-in-Aid for Scientific Research. The authors acknowledge Dr. Mitsuhiko Miyazaki and Ms. Satoko Enomoto for their contribution in the early stage of this work. We also gratefully thank Dr. Michitoshi Hayashi for his encouragement.

References and Notes

(1) Zwier, T. S. *Annu. Rev. Phys. Chem.* **1996**, *47*, 205.
(2) Ebata, T.; Fujii, A.; Mikami, N. *Int. Rev. Phys. Chem*. **1998**, *17*, 331.
(3) Brutschy, B. *Chem. Rev.* **2000**, *100*, 3891.
(4) Kim, K. S.; Tarakeshwar, P.; Lee, J. Y. *Chem. Rev.* **2000**, *100*, 4145.
(5) Chang, H.-C.; Wu, C. C.; Kuo, J.-L. *Int. Rev. Phys. Chem*. **2005**, *24*, 553.
(6) Lisy, J. M. *J. Chem. Phys.* **2006**, *125*, 132302.
(7) Jiang, J.-C.; Wang, Y.-S.; Chang, H.-C.; Lin, S. H.; Lee, Y. T.; Niedner-Schatteburg, G.; Chang, H.-C. *J. Am. Chem. Soc.* **2000**, *122*, 1398.
(8) Miyazaki, M.; Fujii, A.; Ebata, T.; Mikami, N. *Science* **2004**, *304*, 1134.
(9) Shin, J.-W.; Hammer, N. I.; Diken, E. G.; Johnson, M. A.; Walters, R. S.; Jaeger, T. D.; Duncan, M. A.; Christie, R. A.; Jordan, K. D. *Science* **2004**, *304*, 1137.
(10) Wu, C.-C.; Lin, C.-K.; Lee, Y. T.; Chang, H.-C.; Jiang, J.-C.; Kuo, J.-L.; Klein, M. L. *J. Chem. Phys*. **2005**, *122*, 074315.
(11) Kuo, J.-L.; Klein, M. L. *J. Chem. Phys.* **2005**, *122*, 024516.
(12) James, T.; Wales, D. J. *J. Chem. Phys.* **2005**, *122*, 134306.
(13) Iyengar, S. S.; Petersen, M. K.; Day, T. J. F.; Burnham, C. J.; Teige, V. E.; Voth, G. A. *J. Chem. Phys.* **2005**, *123*, 084309.
(14) Burnham, C. J.; Petersen, M. K.; Day, T. J. F.; Iyengar, S. S.; Voth, G. A. *J. Chem. Phys.* **2006**, *124*, 024327.
(15) Singh, N. J.; Park, M.; Min, S. K.; Suh, S. B.; Kim, K. S. *Angew. Chem., Int. Ed.* **2006**, *45*, 3795.
(16) Headrick, J. M.; Diken, E.; Walters, R. S.; Hammer, N. I.; Christie, R. A.; Cui, J.; Myshakin, E. M.; Duncan, M. A.; Johnson, M. A.; Jordan, K. D. *Science* **2005**, *308*, 1765.
(17) Buck, U.; Huisken, F. *Chem. Rev*. **2000**, *100*, 3863.
(18) Pribble, R. N.; Hagemeister, F. C.; Zwier, T. S. *J. Chem. Phys*. **1997**, *106*, 2145.
(19) Narten, A. H.; Habenschuss, A. *J. Chem. Phys*. **1984**, *80*, 3387.
(20) Zang, X.; Yang, X.; Castleman, A. W., Jr. *Chem. Phys. Lett*. **1991**, *185*, 298.
(21) Chang, H.-C.; Jiang, J.-C.; Lin, S. H.; Lee, Y. T.; Chang, H.-C. *J. Phys. Chem. A* **1999**, *103*, 2941.
(22) Chang, H.-C.; Jiang, J.-C.; Chang, H.-C.; Wang, L. R.; Lee, Y. T. *Isr. J. Chem*. **1999**, *39*, 231.
(23) Fujii, A.; Enomoto, S.; Miyazaki, M.; Mikami, N. *J. Phys. Chem. A* **2005**, *109*, 138.
(24) Searcy, J. Q.; Fenn, J. B. *J. Chem. Phys*. **1974**, *61*, 5282.
(25) Wei, S.; Shi, Z.; Castleman, A. W., Jr. *J. Chem. Phys.* **1991**, *94*, 3268.
(26) Frisch, M. J.; Trucks, G. W.; Schlegel, H. B.; Scuseria, G. E.; Robb, M. A.; Cheeseman, J. R.; Montgomery, J. A., Jr.; Vreven, T.; Kudin, K. N.; Burant, J. C.; Millam, J. M.; Iyengar, S. S.; Tomasi, J.; Barone, V.; Mennucci, B.; Cossi, M.; Scalmani, G.; Rega, N.; Petersson, G. A.; Nakatsuji, H.; Hada, M.; Ehara, M.; Toyota, K.; Fukuda, R.; Hasegawa, J.; Ishida, M.; Nakajima, T.; Honda, Y.; Kitao, O.; Nakai, H.; Klene, M.; Li, X.; Knox, J. E.; Hratchian, H. P.; Cross, J. B.; Bakken, V.; Adamo, C.; Jaramillo, J.; Gomperts, R.; Stratmann, R. E.; Yazyev, O.; Austin, A. J.; Cammi, R.; Pomelli, C.; Ochterski, J. W.; Ayala, P. Y.; Morokuma, K.; Voth, G. A.; Salvador, P.; Dannenberg, J. J.; Zakrzewski, V. G.; Dapprich, S.; Daniels, A. D.; Strain, M. C.; Farkas, O.; Malick, D. K.; Rabuck, A. D.; Raghavachari, K.; Foresman, J. B.; Ortiz, J. V.; Cui, Q.; Baboul, A. G.; Clifford, S.; Cioslowski, J.; Stefanov, B. B.; Liu, G.; Liashenko, A.; Piskorz, P.; Komaromi, I.; Martin, R. L.; Fox, D. J.; Keith, T.; Al-Laham, M. A.; Peng, C. Y.; Nanayakkara, A.; Challacombe, M.; Gill, P. M. W.; Johnson, B.; Chen, W.; Wong, M. W.; Gonzalez, C.; Pople, J. A.; *Gaussian 03*, Revision D.01; Gaussian, Inc.: Wallingford, CT, 2004.
(27) Wu, C. C.; Jiang, J. C.; Boo, D. W.; Lin, S. H.; Lee, Y. T.; Chang, H.-C. *J. Chem. Phys*. **2000**, *112*, 176.
(28) Wu, C. C.; Chaudhuri, C.; Jiang, J. C.; Lee, Y. T.; Chang, H.-C. *J. Phys. Chem. A* **2004**, *108*, 2859.
(29) Jiang, J. C.; Chaudhuri, C.; Lee, Y. T.; Chang, H.-C. *J. Phys. Chem. A* **2002**, *106*, 10937.
(30) Suhara, K.; Fujii, A.; Mizuse, K.; Mikami, N.; Kuo, J.-L. *J. Chem. Phys*. **2007**, *126*, 194306.
(31) Solcà, N.; Dopfer, O. *J. Phys. Chem. A* **2005**, *109*, 6174.